Available online at www.sciencedirect.com
SCIENCE DIRECT®
Journal of Molecular Catalysis A: Chemical 214 (2004) 257–264
JOURNAL OF MOLECULAR CATALYSIS A: CHEMICAL
www.elsevier.com/locate/molcata

Catalytic activity of chromium(III), iron(III) and bismuth(III) complexes of 1,2-bis(2-hydroxybenzamido)ethane (H_2hybe) encapsulated in zeolite-Y for liquid phase hydroxylation of phenol

Mannar R. Maurya [a,*], Salam J.J. Titinchi [a], Shri Chand [b]

[a] *Department of Chemistry, Indian Institute of Technology Roorkee, Roorkee 247667, India*
[b] *Department of Chemical Engineering, Indian Institute of Technology Roorkee, Roorkee 247667, India*

Received 4 August 2003; accepted 14 December 2003

Abstract

Iron(III), chromium(III) and bismuth(III) complexes of amidate ligand 1,2-bis(2-hydroxybenzamido)ethane (H_2hybe) encapsulated in the super cages of zeolite-Y have been isolated and characterized by various physico-chemical measurements. 3D model structure generated for $[Fe(hybe)\cdot 2H_2O]^+$ suggests that zeolite-Y can accommodate these complexes in its super cages without any strain. These encapsulated complexes catalyze hydroxylation of phenol using H_2O_2 as oxidant to give catechol as a major and hydroquinone as a minor product. A suitable reaction condition has been optimized for $[Fe(hybe)\cdot 2H_2O]Cl$–Y by considering the effect of various parameters such as concentration of substrate, amount of oxidant and catalysts, reaction time, temperature, and volume of solvent for the maximum hydroxylation of phenol. The results obtained over these new encapsulated catalysts showed that selectivity of the catechol formation is ca. 85%, though transformation of phenol varied in the order $[Fe(hybe)\cdot 2H_2O]Cl$–Y (43.5%) > $[Cr(hybe)\cdot 2H_2O]Cl$–Y (32.8%) > $[Bi(hybe)\cdot 2H_2O]Cl$–Y (30.6%). Catalytic performance of these catalysts has been compared with different metal complexes encapsulated in zeolite-Y.
© 2004 Elsevier B.V. All rights reserved.

Keywords: Oxidation of phenol; Zeolite-Y; Encapsulation; Amidate ligand; Catechol and hydroquinone formation

1. Introduction

The heterogenization of a homogeneous catalyst has been a renewed area of research due to their enhanced activity, selectivity and reusability. Encapsulation of metal complexes, acting as homogeneous catalysts, in the super cages of zeolite matrix provides an ideal solution for the heterogenization. These catalysts, this way, possess the advantages of solid heterogeneous catalysts as well as share many advantageous features of homogeneous catalysts. The metal complexes encapsulated in zeolites find more applications in the synthesis of fine chemicals. These are being used in various types of catalytic reactions e.g. oxidation, alkylation, dehydrogenation, cyclization, amination, acylation, isomerization, rearrangement etc. [1–4] and are able to produce all major industrial products.

The liquid phase hydroxylation of phenol using simple oxidant like molecular oxygen and H_2O_2 is industrially important reaction [5,6]. World wide at least three different processes are in practice where H_2O_2 has been used as an oxidant. However, the major commercial process for the oxidation of phenol by Enichem, Italy uses only zeolite-based catalyst TS-1 [7]. Other two processes involve homogeneous catalysts. Ratnasamy and coworkers [8] and Tatsumi and coworkers [9] have also studied oxidation of phenol with H_2O_2 over TS-1 by considering the effect of various parameters. Applications of TS-1 as catalyst have recently been reviewed by Perego and coworkers [10]. Other types of catalysts have also been tested to enhance the hydroxylation of phenol [11–14]. The catalysts based on zeolite encapsulated metal complexes (ZEMC) have played considerable role in this regard [15–19]. About 90% selectivity towards the formation of catechol has been reported using oxovanadium(IV) complexes of salen (H_2salen = *N*,*N*′-bis(salicylidene)ethane-1,2-diamine) family encapsulated in zeolite-Y [20]. In this work, we have

* Corresponding author. Tel.: +91-1332-285327; fax: +91-1332-273560.
E-mail address: rkmanfcy@iitr.ernet.in (M.R. Maurya).

1381-1169/$ – see front matter © 2004 Elsevier B.V. All rights reserved.
doi:10.1016/j.molcata.2003.12.017

prepared chromium(III), iron(III), and bismuth(III) complexes of 1,2-bis(2-hydroxybenzamido)ethane (H_2hybe, I) encapsulated in zeolite-Y and tested their catalytic activity for the liquid phase hydroxylation of phenol. A suitable reaction condition has been optimized to get maximum hydroxylation.

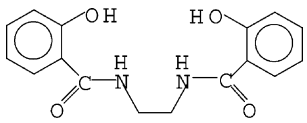

I: H_2hybe

2. Experimental

2.1. Materials

Analytical reagent grade metal nitrates (nitrates of Cr(III), Fe(III), and Bi(III)), 30% aqueous H_2O_2 and phenol were obtained from Qualigens, India. Methylsalicylate and 1,2-diaminoethane were procured from E. Merck, India. Zeolite-Y (Si/Al ∼10) was obtained from Indian Oil Corporation (R&D), Faridabad, India. All other chemicals and solvents used were of AR grade. 1,2-Bis(2-hydroxybenzamido)ethane (H_2hybe) was prepared as described by Dash and Mishra [21].

2.2. Preparations

2.2.1. Preparation of metal exchanged zeolite, M–Y [M=Cr(III), Fe(III), and Bi(III)]

About 5.0 g of Na–Y zeolite was suspended in 300 ml distilled water, which contained 50 mol of metal nitrate [nitrates of Cr(III), Fe(III) or Bi(III)]. The reaction mixture was heated while stirring at ca. 90 °C for 24 h. The solid was filtered, washed with hot distilled water till the filtrate was free from any free metal ion on the surface of the zeolite and then dried for 15 h at 150 °C in air.

2.2.2. Preparation of [M(hybe)·2H_2O]Cl–Y [M=Cr(III), Fe(III), and Bi(III)]

The encapsulated complexes were prepared by general method. About 1.0 g M–Y and 2.5 g H_2hybe were mixed in a 50 ml MeCN in a round bottom flask and the reaction mixture was heated at reflux for ca. 15 h while stirring in an oil bath. After cooling, the slurry was Soxhlet extracted with methanol (ca. 48 h) till the complex was free from unreacted ligand and any free metal complex on the surface of the zeolite. Finally this was treated with aqueous 0.01 M solution of NaCl for 8 h. The encapsulated complexes were filtered, washed with hot distilled water till no precipitation of AgCl was observed on treating filtrate with $AgNO_3$ solution. The colored (colorless in case of Bi(III)) solid was dried at 150 °C for several hours to constant weight.

2.3. Physical methods and analysis

The metal contents were measured using GBC Avanta Atomic Absorption Spectrometer. Thermogravimetric analyses of the catalysts were carried out using TG Stanton Redcroft STA 780 instrument. X-ray diffractograms of solid catalysts were recorded using Philips PW 1140/90 X-ray powder diffractometer with Cu Kα target at the Institute Instrumentation Center. IR spectra were recorded as KBr pellet on a Perkin-Elmer model 1600 FT-IR spectrometer. Electronic spectra were recorded in Nujol on a Shimadzu 1601 UV-Vis spectrophotometer by layering mull of sample to inside of one of the cuvette while keeping another one layered with Nujol as reference. All catalyzed reaction products were analyzed using Nucon 5700 gas chromatograph fitted with FID detector, a 2 m × 2 mm (i.d.) OV-17 (S.S.) column and ORACLE 2 computer software. Scanning electron micrographs of catalysts were recorded on a Leo instrument (model 435 VP). The samples were dusted on alumina and coated with a thin film of gold to prevent surface changing and to protect the surface material from thermal damage by the electron beam. In all analyses a uniform thickness of about 0.1 mm was maintained.

2.4. Catalytic activity study: hydroxylation of phenol

The catalytic hydroxylation of phenol was carried out in a 50 ml flask fitted with a water circulated condenser. In a typical reaction, an aqueous solution of 30% H_2O_2 (5.67 g, 0.05 mol) and phenol (4.7 g, 0.05 mol) were mixed in 2 ml of MeCN and the reaction mixture was heated at 80 °C with continuous stirring in an oil bath. An appropriate catalyst (0.025 g) was added to the reaction mixture and the reaction was considered to begin. During the reaction, the products were analyzed after specific interval of time using a gas chromatograph by withdrawing small aliquot. The effects of various parameters, such as amounts of substrate, oxidant, and catalyst as well as the temperature of the reaction were studied in order to see their effect on the reaction product pattern.

3. Results and discussion

3.1. Synthesis and characterization of catalysts

The synthesis of Cr(III), Fe(III), and Bi(III) complexes encapsulated in super cages of zeolite-Y was carried out by a flexible ligand method which involves the reaction of MeCN solution of ligand with pre-metal exchanged zeolite, M–Y. The solvent MeCN facilitated the insertion of ligand due to its flexible nature in the cavity of the zeolite followed by complexation with metal ions. Complexation of H_2hybe with Cr(III) and Fe(III) ions were accompanied by the color change, while Bi(III) gave colorless compound. Soxhlet extraction with methanol purified the crude

Table 1
Chemical composition, physical and analytical data

Serial number	Compound	Color	Metal content (wt.%)	Number of metal per unit cell
1	Fe–Y	Brown	0.55	1.6
2	Cr–Y	Green	1.67	5.3
3	Bi–Y	White	2.17	1.7
4	[Fe(hybe)·2H_2O]Cl–Y	Pale brown	0.31	0.9
5	[Cr(hybe)·2H_2O]Cl–Y	Light green	1.14	3.6
6	[Bi(hybe)·2H_2O]Cl–Y	White	1.06	0.8

mass and removed excess ligand as well as metal complex formed, if any, on the surface of the zeolite due to leaching. The remaining uncomplexed metal ions in the zeolite were removed by exchanging with aqueous 0.01 M NaCl solution. The percentage of metal contents determined before and after encapsulation by atomic absorption spectrometry (AAS), estimated number of metal molecules per unit cell along with their expected formula and color are presented in Table 1. As crude mass was extracted with methanol, the metal ion content found after encapsulation is only due to the presence of metal complexes in the super cages of the zeolite-Y. The formula of the complexes are based on the iron(III) complex [Fe(hybe)·2H_2O]Cl which has been characterized by Dash and Mishra [21]. We also expect Cl^- as counter ion in all these catalysts as crude mass was treated with conc. NaCl solution as noted above. The scanning electron micrographs (SEM) of the metal exchanged zeolite and their respective encapsulated complexes indicate the presence of well defined crystals free from any shadow of the metal ions or complexes present on their external surface.

3.2. IR spectral studies

A partial list of IR spectral data of ligand and its encapsulated complexes are presented in Table 2. The ligand exhibits a broad band in the 2300–2600 cm^{-1} region due to intra-molecular hydrogen bonding between phenolic and amide C=O. Absence of this band in the spectra of encapsulated complexes suggests the breaking of hydrogen bonding followed by deportation of the phenolic oxygen and coordination to the metal ion. The ligand also exhibits three sharp peaks at 1641, 1547, and 1252 cm^{-1} due to amide-I, II, and III modes, respectively. Amide-I band arises due to ν(C=O) mode while amide-II and III arise due to ν(C–N) (stretching) and ν(NH) (bending) modes, respectively. The amide-II band could not be located due to the presence of strong Si–O band in this region while other two bands register low frequency shift in the spectra of the encapsulated complexes, indicating the coordination of amide nitrogen to the metal ion. This is supplemented by the lower frequency shift of ν(NH) peak, which appears at 3377 cm^{-1} in free ligand. The coordination of amide –NH group has been confirmed in several oxovanadium(IV) complexes [22]. The appearance of five bands in the low frequency region (400–500 cm^{-1}) further indicates the coordination of nitrogen and oxygen to the metal. Thus, IR spectra support ONNO donor dibasic tetradentate behavior of H_2hybe.

3.3. Electronic spectral studies

The electronic spectrum of ligand exhibits two bands at 306.5 and 240 nm due to n–π^* and π–π^* transitions of the phenolic group, respectively. In catalysts, these bands appear at higher nm range (Table 2), which suggest the association of ligand with metal ions. In addition, all these catalysts display a band at 206–207.5 nm which seems to be ϕ–ϕ^* transition due to the presence of benzene ring. The band due to d–d transitions in Fe(III) and Cr(III) base catalysts could not be located in Nujol. The electronic spectral data of the catalysts along with the ligand are also presented in Table 2 and spectra of the catalysts are reproduced in Fig. 1.

3.4. Powder X-ray diffraction studies

The powder X-ray diffraction patterns of Na–Y, M–Y and encapsulated metal complexes were recorded at 2θ values between 5 and 70. The XRD patterns of encapsulated complexes are presented in Fig. 2. An essentially similar pattern in Na–Y, M–Y and encapsulated metal complexes was noticed, though slight change in the intensity of the bands in encapsulated complexes is in line. These observations indicate that the framework of the zeolite has not undergone any significant structural change during incorporation of the catalysts i.e. crystallinity of the zeolite-Y is preserved during encapsulation. No new peaks due to neat complex was detected in the encapsulated zeolite due to probably very low percent loading of metal complexes.

Table 2
IR and electronic spectra of ligand and encapsulated complexes

Compound	IR frequency (cm^{-1})			λ_{max} (nm)
	Amide-I	Amide-II	ν(M–N)/(M–O)	
H_2hybe[a]	1641	1547	–	240, 306.5
[Fe(hybe)·2H_2O]Cl–Y	1620	1487	432,451,480,496,515	206, 248, 316
[Cr(hybe)·2H_2O]Cl–Y	1615	1495	411,438,462,478,497	206, 250, 317.5
[Bi(hybe)·2H_2O]Cl–Y	1620	1496	407,427,452,486,510	207.5, 250, 310

[a] Electronic spectrum recorded in methanol.

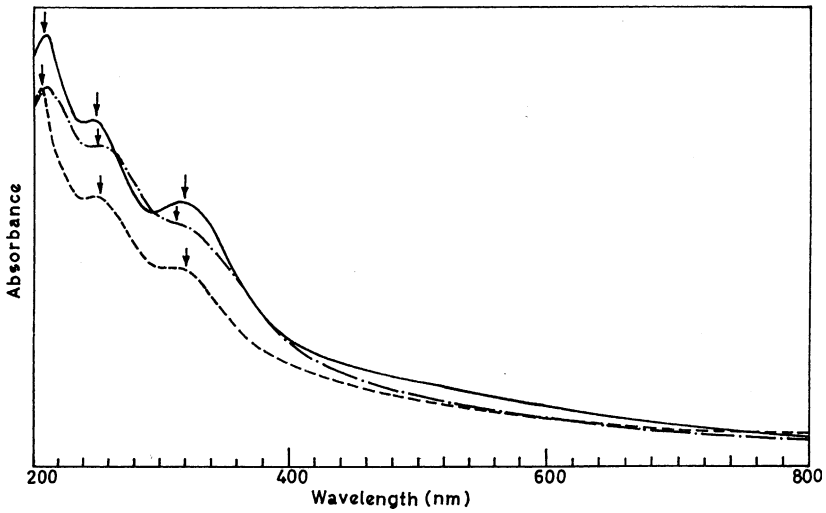

Fig. 1. Electronic spectra of catalysts [Cr(hybe)·2H$_2$O]Cl–Y (–·–·–), [Fe(hybe)·2H$_2$O]Cl–Y (—) and [Bi(hybe)·2H$_2$O]Cl–Y(---).

3.5. Thermogravimetric studies

Encapsulation of metal complexes in the zeolite-Y was further supported by their thermal analysis patterns. The weight loss of these catalysts occurs in two major stages in the broad temperature range. First stage weight loss starts at ca. 150 °C and completes at ca. 350 °C. This loss is due to removal of intra-zeolite water and Cl^- ion as well as water associated with encapsulated complex as only intra-zeolite water would loss at relatively lower temperature range. The decomposition of ligand occurs in the second stage, which starts immediately after first stage and completes at ca. 605 °C. Unfortunately, it is difficult to estimate loss percent in both stages separately due to overlapping of the two steps.

3.6. 3D molecular model structure

The three-dimensional model structure for [Fe(hybe)·2H$_2$O]$^+$ was created using CS Chem 3D Ultra molecular modeling and analysis programme [23]. Fig. 3 presents the model structure and selected bond lengths and bond angles are given along with figure caption. The observed bond lengths and bond angles are close to the optimal values. It is clear from the figure that Fe(III) acquires distorted octahedral structure where one of the phenolic oxygen and

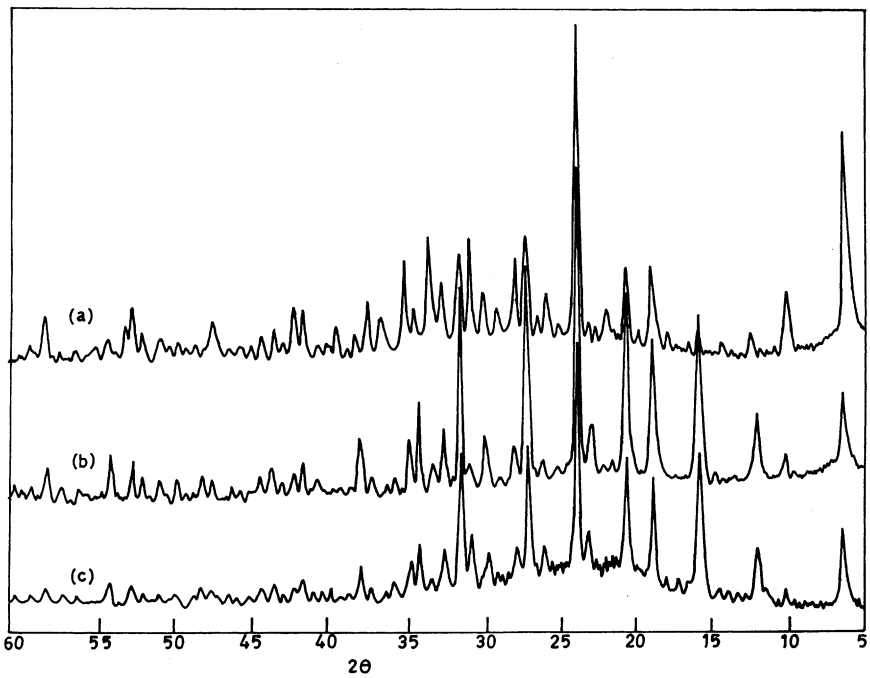

Fig. 2. XRD patterns of (a) [Cr(hybe)·2H$_2$O]Cl–Y, (b) [Fe(hybe)·2H$_2$O]Cl–Y, and (c) [Bi(hybe)·2H$_2$O]Cl–Y.

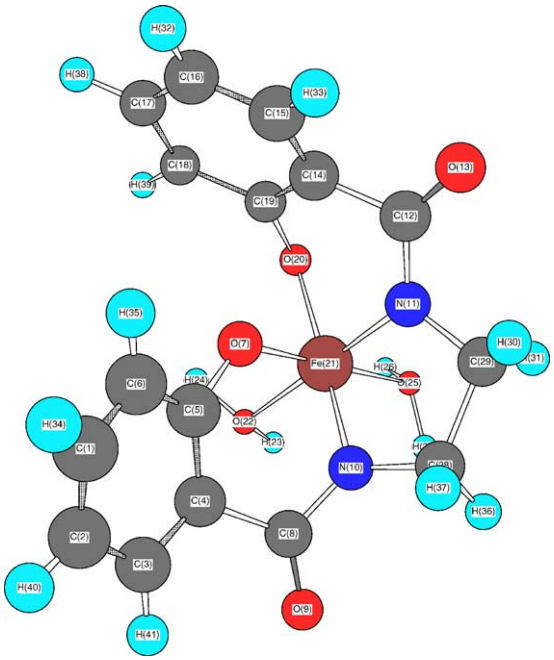

Fig. 3. 3D model structure of $[Fe(hybe)\cdot 2H_2O]^+$; bond length (Å): Fe–O(20), 1.81; Fe–N(10), 1.846; Fe–N(11), 1.846; Fe–O(22), 1.81; Fe–O(25), 1.81; N(10)–H(28), 1.028; N(11)–H(29), 1.028. Bond angle (°): O(7)–Fe–N(10), 83.225; O(7)–Fe–N(11), 94.449; O(7)–Fe–O(20), 89.999; O(7)–Fe–O(22), 89.999; O(7)–Fe–O(25), 180; O(20)–Fe–N(11), 92.326; O(20)–Fe–N(10), 175.545; O(20)–Fe–O(22), 90; O(20)–Fe–O(25), 90; N(10)–Fe–N(11), 87.977; N(10)–Fe–O(22), 87.167; N(10)–Fe–O(25), 96.776; N(11)–Fe–O(22), 175.552; N(11)–Fe–O(25), 85.552; O(22)–Fe–O(25), 90.

amido nitrogen are in the axial positions and are *trans* to each other with bond angle of 177.08 Å. Other oxygen and nitrogen of the ligand and oxygen of water molecules are in the equatorial positions. The diagonal distance of the structure is less than 10 Å and this suggests that zeolite-Y can accommodate $[Fe(hybe)\cdot 2H_2O]^+$ in its super cages without putting any strain.

3.7. Catalytic activity

The catalytic hydroxylation of phenol using three different catalysts viz. $[Fe(hybe)\cdot 2H_2O]Cl$–Y, $[Cr(hybe)\cdot 2H_2O]Cl$–Y and $[Bi(hybe)\cdot 2H_2O]Cl$–Y and H_2O_2 as oxidant in acetonitrile was studied as a function of time. The two products catechol and hyrdoquinone, as shown by Eq. (1), were observed with a mass balance of >95%. Other products, if any, present as minor constituents could not be detected by the gas chromatography under the conditions used herein and were neglected. During catalytic oxidation, the encapsulated complexes react with H_2O_2 to give peroxo intermediate complexes, which ultimately transfer oxygen to the substrate. In order to achieve suitable reaction conditions for the maximum hydroxylation of phenol, the following parameters were considered in detail using $[Fe(hybe)\cdot 2H_2O]Cl$–Y as representative catalyst:

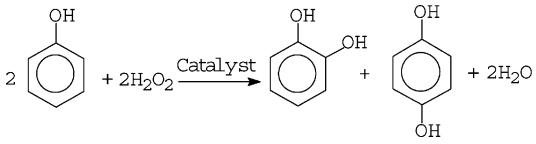

3.7.1. Effect of temperature

In order to study the variation in catalytic performance three different temperatures 50, 65, and 80 °C were selected while keeping other parameters fixed (i.e. 4.7 g phenol, 5.67 g H_2O_2, 0.025 g catalyst in 2 ml MeCN). The results presented in Fig. 4 show that reaction temperature of 80 °C gives the maximum hydroxylation of phenol (ca. 43%), whereas, the percentage phenol hydroxylation at 65 and 50 °C are lower (32 and 23%, respectively). The best performance at 80 °C also has an added advantage with maximum (steady state) percentage transformation in a shorter duration of 1 h.

3.7.2. Effect of amount of catalyst

Amount of catalyst also has influence on the percentage of phenol hydroxylation. Fig. 5 represents the details of such effect. As shown in the figure, increasing the amount of catalyst from 5 to 25 mg enhanced the phenol conversion from 32 to 42%, and ca. 90% of the total conversion was achieved in the initial 1 h. Further increment of catalyst amount to

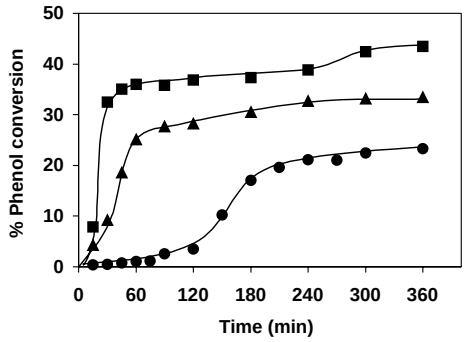

Fig. 4. Effect of temperature on phenol oxidation: (●) 50 °C; (▲) 65 °C; (■) 80 °C.

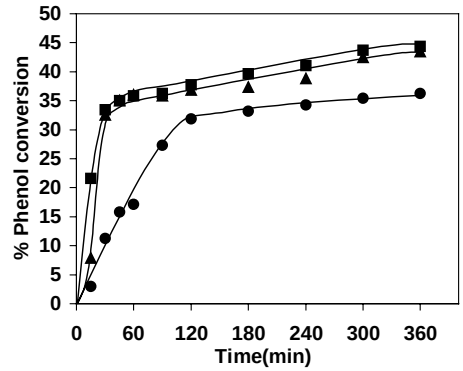

Fig. 5. Effect of catalyst weight on phenol oxidation: (●) 5 mg; (▲) 25 mg; (■) 40 mg.

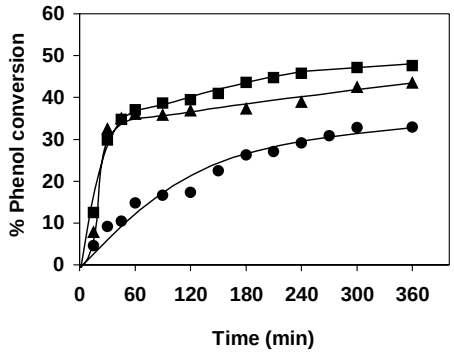

Fig. 6. Effect of H_2O_2 concentration (phenol:H_2O_2 ratio) on phenol oxidation: (■) 0.025 mol (1:0.5); (▲) 0.05 mol (1:1); (■) 0.1 mol (1:2).

40 mg resulted in only a marginal increase (ca. 43%) in percent substrate conversion. This has been interpreted in terms of thermodynamic and mass transfer limitations at higher reaction rate. In all cases reaction acquires steady state in ca. 6 h.

3.7.3. Effect of H_2O_2 concentration

The influence of concentration on the oxidation of phenol as a function of time is presented in Fig. 6. Three different H_2O_2:phenol molar ratios (0.5:1, 1:1, and 2:1) were used in this study. It is evident from the plot that 1:1 and 2:1 molar ratio gave relatively good conversion of phenol (48 and 53%, respectively), while the percent H_2O_2 efficiency in 1:1 molar ratio is much higher than in 2:1 molar ratio. The 0.5:1 (H_2O_2:phenol) molar ratio gave only 30% phenol conversion with H_2O_2 efficiency of ca. 64%. On comparing these results it is clear that 1:1 (H_2O_2:phenol) molar ratio is the suitable molar ratio for the better performance of catalyst with reasonable percentage H_2O_2 efficiency and large concentration of oxidant is not an essential condition to maximize phenol conversion. With 2:1 (H_2O_2:phenol) molar ratio a small amount (∼2%) *p*-benzoquinone is also formed and this is probably due to further oxidation of hydroquinone.

3.7.4. Effect of phenol concentration

To study the influence of initial moles of phenol (substrate), three different amounts of phenol 2.35, 4.7, and 9.4 g were used, while keeping all other parameters fixed (5.67 g H_2O_2, 0.025 g catalyst, 2 ml MeCN at 80 °C). It is clear from the results shown in Fig. 7 that with 1:1 (PhOH:H_2O_2) molar ratio (4.7 g PhOH) a maximum of 48% conversion, and with 1:2 molar ratio a maximum of 53% phenol conversion were obtained. Increasing the amount of PhOH (i.e. 2:1 (PhOH:H_2O_2) molar ratio) lowered the conversion to 32%. However, comparing efficiencies for these ratios, it is clear that 1:1 molar ratio is the best ratio to obtain maximum percent conversion with a reasonable percent H_2O_2 efficiency. This conclusion is in the agreement with the observation obtained for the effect of H_2O_2 concentration.

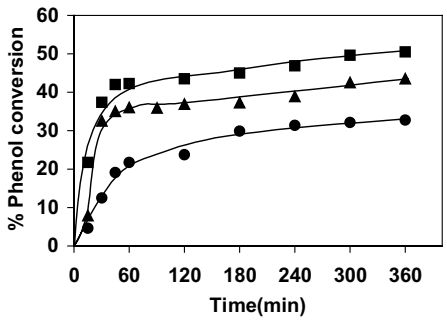

Fig. 7. Effect of phenol concentration (phenol:H_2O_2 ratio) on phenol oxidation: (■) 0.025 mol (0.5:1); (▲) 0.05 mol (1:1); (●) 0.1 mol (2:1).

3.7.5. Effect of amount of solvent

The influence of the volume of solvent (MeCN) on the reaction is illustrated in Fig. 8. It is evident that the volume of acetonitrile plays an important role on the percentage conversion. The performance with 2 ml of solvent was found to be the best under reaction conditions with 43% phenol conversion. Increasing the volume of solvent to 4 or 6 ml, decreases the percent phenol conversion (35 or 28%, respectively). It was also observed that less than 2 ml MeCN was not sufficient enough to dissolve the reaction mixture to give a homogeneous medium.

3.8. Catalytic activity of other catalysts and proposed mechanism

After acquiring the best suited reaction conditions by considering the catalyst [Fe(hybe)·2H_2O]Cl–Y as a representative catalyst, the other two catalysts viz. [Cr(hybe)·2H_2O]Cl–Y and [Bi(hybe)·2H_2O]Cl–Y were studied under similar condition (i.e. 0.05 mol of phenol, 5.67 g H_2O_2, 0.025 g catalyst in 2 ml of CH_3CN at 80 °C) for comparison. The performance of these catalysts as a function of time is presented in Fig. 9. It is clear from the figure that Fe(III)-based catalyst is not only catalytically more active by showing highest conversion of phenol but also reaches to the steady state in just 1 h. The Cr(III)-based catalyst takes a longer time to start and reaches steady state in 3 h with the performance poorer (ca. 33%) than the Fe(III)-based catalyst. Induction period in the plot for this

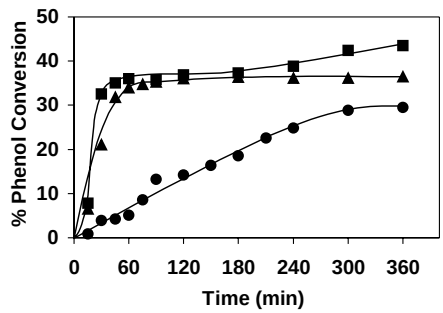

Fig. 8. Effect of volume of solvent: (●) 6 ml; (▲) 4 ml; (■) 2 ml.

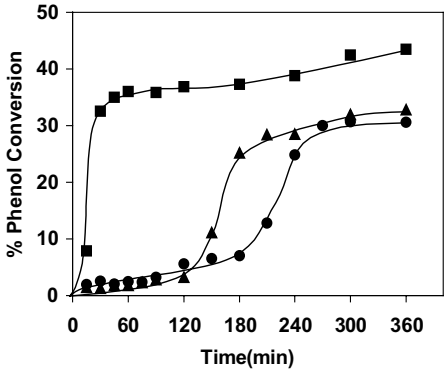

Fig. 9. Kinetic plots of percentage phenol conversion: (▲) [Cr(hybe)·$2H_2O$]Cl–Y, (■) [Fe(hybe)·$2H_2O$]Cl–Y, (●) [Bi(hybe)·$2H_2O$]Cl–Y.

catalyst indicates either slow formation of peroxo species or taking longer time to transfer oxygen to the substrate due to mass transfer limitations. The percent conversion is only about 23% with Bi(III)-based catalyst and requires ca. 4 h to reach the steady state. Thus, the order of performance of these catalysts are: [Fe(hybe)·$2H_2O$]Cl–Y > [Cr(hybe)·$2H_2O$]Cl–Y > [Bi(hybe)·$2H_2O$]Cl–Y. A further increment of hydroxylation fails even by varying various parameters and it appeared to be influenced by clogging of the pore system of zeolite with reaction products [24]. As color of the reaction mixture in the experiment carried out here is light brown, the formation of a small amount of polymeric material seems to be likely. The poisoning of the catalyst by such polymeric product may also arise, as these materials would create partial hindrance for substrate in approaching the catalyst sitting in the cavity of zeolite [25]. The reported range of percent phenol hydroxylation using various zeolite-encapsulated catalysts is 5–35. Interestingly, recycled catalysts after regeneration exhibit almost similar catalytic activity and this observation supports above factors for limiting the conversion of phenol during catalytic hydroxylation.

Table 3
Percent selectivity of catechol and hydroquinone formation and percent conversion of phenol after 6 h of reaction time

Catalyst	Percent phenol conversion	Percent selectivity	
		Catechol	Hydroquinone
[Fe(hybe)·$2H_2O$]Cl–Y	43.47	88.0	12.0
[Cr(hybe)·$2H_2O$]Cl–Y	32.81	90.0	10.0
[Bi(hybe)·$2H_2O$]Cl–Y	30.58	85.0	15.0

The metal complexes encapsulated in zeolite-Y have been reported to yield catechol in much higher proportion in comparison to hydroquinone. The product selectivity of such molecular sieve based catalysts is based on the shape and size of the product molecule. In terms of the formation of catechol and hydroquinone, all these catalysts reported here are also highly selective towards the formation of catechol and least selective for hydroquinone after 6 h of reaction time. Table 3 summarizes these results for phenol conversion after 6 h of reaction time and Fig. 10 presents these results as a bar diagram. It is clear from the table that the selectivity of catechol formation is comparable (85–90%) in all cases though transformation of phenol varied from catalyst to catalyst. Interestingly, this high selectivity of catechol formation is maintained even after 24 h of reaction time.

Leaching or decomposition of the catalysts was tested by considering blank reaction i.e. using 5.67 g H_2O_2, 0.025 g catalyst in 2 ml of CH_3CN at 80 °C for 6 h. Absence of metal ions in mother liquor suggests no leaching or decomposition of complexes during catalytic activity. Recovered catalysts are also reusable after regeneration. For example [Fe(hybe)·$2H_2O$]Cl–Y, a representative catalyst was reused for phenol hydroxylation after its regeneration. Comparable catalytic activity of recovered catalyst suggests its reusability. Comparable IR and electronic spectral patterns of fresh and used catalysts also suggest their further reusability.

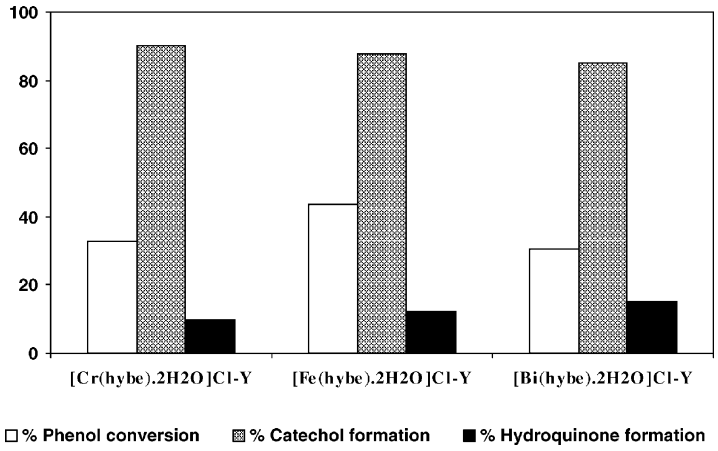

Fig. 10. Bar diagram showing phenol conversion and catechol and hydroquinone formation for various catalysts.

As *m*-dihydroxybenzene is not detected in the product mixture, the involvement of hydroxyl radical as direct oxidizing agent is unlikely. The hydroxylation of phenol may involve the coordination of oxygen atoms at the vacant sites of metal atom in the complex to form peroxo species [17]. This intermediate transfers the coordinated oxygen atoms to the substrates to obtain the product. All these catalysts reported here can extend the vacant sites easily for peroxo species formation. Thus, the catalytic performance of the encapsulated complexes could be attributed to the formation of facile and reversible intermediate species. The hydroxylation of phenol may also proceed by an eletrophilic substitution mechanism that is common for the hydroxylation of phenol catalyzed by strong acids or organic peracids [26]. Masri and Hronec [27] have suggested the formation of an intermediate ionic species $[M(Pc)(HOOH)^{+}]$ in case of phthalocyanine. The activated hydrogen peroxide or peroxo metal complexes undergo heterolysis at the O–O bond and produce the ionic OH^{+} attacking species which in turn hydroxylate phenol via an electrophilic substitution mechanism at the *ortho* and *para* positions. The difference in the reactivity of the catalysts reported here is, thus, related to their ability to form intermediate acidic species.

4. Conclusions

Iron(III), chromium(III), and bismuth(III) complexes of H_2hybe have been encapsulated in the super cages (α-cages) of zeolite-Y. Spectroscopic studies, chemical analysis, SEM, and XRD as well as thermogravimetric patterns provide a clear evidence for their encapsulation. These encapsulated complexes catalyze the hydroxylation of phenol to a mixture of catechol and hydroquinone in moderate yield and follow the order [Fe(hybe)·2H_2O]Cl–Y > [Cr(hybe)·2H_2O]Cl–Y > [Bi(hybe)·2H_2O]Cl–Y. Their catalytic activities are only due to encapsulated complexes as no leaching of metal ions or metal complexes were detected in solution when blank reaction was carried out using 5.67 g H_2O_2, 0.025 g catalyst in 2 ml of MeCN at 80 °C for several hours. Several factors such as amount of oxidant, catalyst, volume, and type of solvents and temperature of the reaction mixture affect the performance of these catalysts. Under the best-suited reaction conditions, the selectivity of catechol formation is 85–90% with these catalysts. Such high selectivity has only been noticed with oxovanadium(IV) complexes of H_2salen family [20]. Comparable IR and electronic spectral patterns of fresh and used encapsulated catalysts suggest that these can be used further for catalytic study.

Acknowledgements

Authors are thankful to Prof. R.C. Maurya, Department of Chemistry, R.D. University, Jabalpur, for providing model structure and other calculations appearing in this paper. SJJT is thankful to the Indian Council of Cultural Relations (ICCR), New Delhi for fellowship.

References

[1] K.K. Fodor, G.A. Sebastiaan, R.A. Sheldon, Enantiomer 4 (1999) 497. CAN 132:222038.
[2] G.J. Hutchings, Chem. Commun. (1999) 301.
[3] J.S. Rafelt, J.H. Clark, Catal. Today 57 (2000) 3, and references therein.
[4] R.A. Sheldon, I.W.C.E. Arends, A. Dijksman, Catal. Today 57 (2000) 157.
[5] R.A. Sheldon, R.A. Vansanten, Catalytic Oxidation: Principles and Applications, World Scientific, Singapore, 1995.
[6] Industrial Organic Chemicals: Starting Materials and Intermediates, An Ullamann's Encyclopaedia, vol. 6, Wiley-VCH, New York, 1999.
[7] M. Taramasso, G. Perego, B. Notari, U.S. Patent 4,410,501 (1983) to Sanamprogetti, M. Taramasso, G. Manara, V. Fattore, B. Notari, U.S. Patent 4,666,692 (1987) to Sanamprogetti.
[8] A. Thangaraj, R. Kumar, P. Ratnasamy, J. Catal. 131 (1991) 294.
[9] T. Yokoi, P. Wu, T. Tatsumi, Catal. Commun. 4 (2003) 11.
[10] C. Perego, A. Carati, P. Ingallina, M.A. Mantegazza, G. Bellussi, Appl. Catal. A: Gen. 221 (2001) 63.
[11] V. Rives, A. Dube, S. Kannan, Phys. Chem. Chem. Phys. 3 (2001) 4826.
[12] H. Zhang, X. Zhang, Y. Ding, L. Yan, T. Ren, J. Suo, New J. Chem. 26 (2002) 376.
[13] R.J. Mahalingam, S. Bodamali, P. Selvam, Chem. Lett. 11 (1999) 1141.
[14] K. Takai, Y. Shimashaki, T. Shishido, K. Takehira, Bull. Chem. Soc. Jpn. 75 (2002) 311.
[15] K.J. Balkus Jr, A.G. Gabrielov, J. Inclusion Phenom. Mol. Recognit. Chem. 21 (1989) 159.
[16] R. Raja, P. Ratnasamy, Stud. Surf. Sci. Catal. 101 (1996) 181.
[17] C.R. Jacob, S.P. Varkey, P. Ratnasamy, Microporous Mesoporous Mat. 22 (1998) 465.
[18] T. Joseph, C.S. Sajanikumari, S.S. Deshpade, S. Gopinathan, Indian J. Chem. 38A (1999) 792.
[19] S. Seelan, A.K. Sinha, D. Srinivas, S. Sivasanker, Bull. Catal. Soc. India 1 (2002) 29.
[20] M.R. Maurya, M. Kumar, S.J.J. Titinchi, H.S. Abbo, S. Chand, Catal. Lett. 86 (2003) 97.
[21] A.C. Dash, A. Mishra, Indian J. Chem. 37A (1998) 961.
[22] M.R. Maurya, Coord. Chem. Rev. 237 (2003) 163.
[23] C.S. Chem 3D Ultra Molecular Modeling and Analysis, Cambridge, http://www.cambridgesoft.com.
[24] F. Bedioui, Coord. Chem. Rev. 144 (1995) 39.
[25] J. Sun, X. Meng, Y. Shi, R. Wang, S. Feng, D. Jiang, R. Xu, F.-S. Xiao, J. Catal. 193 (2000) 199.
[26] R.A. Sheldon, J.K. Kochi, Metal-Catalysed Oxidations of Organic Compounds, Academic Press, New York, 1981.
[27] Y. Masri, M. Hronec, Stud. Surf. Sci. Catal. 66 (1991) 455.